Journal of Molecular Catalysis A: Chemical 338 (2011) 65–70

Contents lists available at ScienceDirect

Journal of Molecular Catalysis A: Chemical

journal homepage: www.elsevier.com/locate/molcata

Antibacterial activity of Nb–aluminum oxide prepared by the non-hydrolytic sol–gel route

C. dos S. Alfenas[a], G.P. Ricci[a], E.H. de Faria[a], M. Saltarelli[a], O.J. de Lima[a], Z.N. da Rocha[b], E.J. Nassar[a], Paulo S. Calefi[a], Lilian B. Montanari[a], Carlos H. Gomes Martins[a], Katia J. Ciuffi[a,*]

[a] Universidade de Franca, Av. Dr. Armando Salles Oliveira, Parque Universitário, 201, 14404-600, Franca, SP, Brazil
[b] Universidade Federal da Bahia, Instituto de Química, Departamento de Química Geral e Inorgânica, Campus de Ondina, 40170-290, Salvador, BA, Brazil

ARTICLE INFO

Article history:
Received 15 August 2010
Received in revised form 19 January 2011
Accepted 25 January 2011
Available online 2 March 2011

Keywords:
Sol–gel
Non-hydrolytic
Nb–aluminum oxide
Antibacterial activity

ABSTRACT

Brazil has been the largest producer of niobium (Nb_2O_5) since 1980, and this material is usually applied to reduce corrosion in alloys. In addition, it has recently been evaluated for use in other technological areas, such as adsorption and catalysis. This paper presents the results of the antibacterial activity of Nb–aluminum oxide, designated MAC–Nb^{5+}, prepared by the non-hydrolytic sol–gel route. The resulting material MAC–Nb^{5+} was characterized by several techniques including X-ray diffraction, thermal analysis, infrared absorption spectroscopy, differential pulse voltammetry, surface area measurements, and scanning electron microscopy. The displacements of the bands due to Al–O and Al–OH in the infrared spectra of MAC–Nb^{5+} in relation to alumina confirmed the coordination of Nb^{5+} ions to the surface and inside the pores of the alumina matrix. The powder XRD of MAC–Nb^{5+} suggested that the material is amorphous and that the niobium oxide is well-dispersed over the alumina matrix. Differential pulse voltammetry revealed the redox process that involves Nb–O–Al. Results from the biological assays for determination of the antibacterial activity of MAC–Nb^{5+} were obtained by the following methodologies: determination of the minimum inhibitory concentration and antibacterial activity assay by agar diffusion. It was observed that MAC–Nb^{5+} displays antibacterial activity against all the tested bacteria.

1. Introduction

Applications of antibacterial materials have recently attracted great interest due to the worldwide concern about public health [1]. Inorganic antibacterial activity has been observed for several metal ions dispersed in many types of matrices. Indeed, various ions such as Ag^+, Cu^{2+}, Fe^{3+}, Zn^{2+} and Nb^{5+} dispersed in such different matrices as clays, alumina and silica, by various methodologies, have been employed. Some inorganic matrices such as zeolites, clays, apatite, phosphates, titanium oxides and glasses have also been used [2,3].

In this context, the sol–gel methodology has attracted a lot of attention from countless scientific and technological areas, due to the possibility of inserting metallic ions via their coordination to the surface of the support or their entrapment in the interior of matrix pores, thereby giving rise to materials with distinct morphologies, structures and chemical and biological characteristics for different applications. The material properties depend on the ability of the dispersed metallic ion to interact with the reactive medium.

Our research group has recently, prepared alumina and aluminosilicate matrices doped with cobalt ions by the non-hydrolytic sol–gel route [4,5]. Although this route has been less reported than the traditional hydrolytic method, it frequently allows better control of the material's properties, such as morphology. This is because in the hydrolytic sol–gel route the hydrolysis and condensation reactions generally take place at reaction rates that are too fast, thereby resulting in loss of property control over the obtained material [6].

The isomorphic substitution of Al^{3+} ions in alumina matrices with metals like Nb^{5+} is responsible for the generation of new active sites on the surface of the material. This makes alumina–Nb^{5+} good candidates for the adsorption or fixation of metals, viruses, bacteria and other harmful substances onto their surface. In addition, due to their low cost and favorable thermal stability, alumina matrices can be used as excellent carriers for the synthesis of antibacterial materials.

Inorganic antibacterial agents have various industrial applications in environmental, food, synthetic textiles, packaging, healthcare, and medical care products. In this sense, aluminum

* Corresponding author.
E-mail address: ciuffi@unifran.br (K.J. Ciuffi).

1381-1169/$ – see front matter © 2011 Elsevier B.V. All rights reserved.
doi:10.1016/j.molcata.2011.01.026

oxide nanoparticles and aluminum oxide nanoparticles modified with some metallic ions have a wide range of utilizations in both industrial and personal care products. Sadiq et al. [7] have recently reported a study on the antibacterial activity of aluminum oxide against Gram-negative bacteria. According to these authors, their antibacterial activity is known to be a function of the surface area in contact with the bacteria. This is because a larger surface area promoted adsorption and reactions with bio-organics on the matrix surface [7].

The present work reports on optimized conditions for the preparation of an alumina matrix containing niobium in the powder form. This material was obtained by a non-hydrolytic sol–gel route via condensation of aluminum chloride with diisopropyl ether, in the presence of the niobium precursor. The obtained xerogel was dried at 175 °C and characterized by several techniques. The antibacterial activity of the material was also evaluated against standard strains found in the oral cavity.

2. Experimental

All solvents and reagents were of analytical grade (Merck and Aldrich) unless otherwise stated. Dichloromethane (DCM) was suspended on anhydrous $CaCl_2$ for 2.5 h, filtered, distilled over P_2O_5 and kept over 0.4 nm molecular sieves.

2.1. Synthesis of Nb–alumina

Nb-precursor – the precursor was prepared by reaction of potassium niobate ($K_8Nb_6O_{19}$) with hydrochloric acid. Gels were prepared in oven-dried glassware. The solid material was synthesized via modification of the method previously described in the literature and modified by us [4,5,8,9]. Anhydrous aluminum chloride ($AlCl_3$, 14 g, 0.105 mol), diisopropyl ether ($^iPr_2O$, 35 mL, 0.248 mol) and the niobium precursor (150 mg) were reacted with methanol in dry DCM (120 mL, previously distilled), under reflux at 110 °C and argon atmosphere. A gel was formed after 4 h of reaction. After reflux, the mixture was cooled and aged overnight in the mother liquor, at room temperature. Then, the solvent was removed under vacuum. The solid, designated hereafter MAC–Nb^{5+}, was washed with several solvents in the following order: DCM, acetonitrile and methanol, and dried at 175 °C for 70 min.

Control reactions, or blank tests, were conducted with the alumina matrix containing no niobium, which was prepared in the same way as the Nb precursor, but in the absence of the niobium ions.

Thermal analyses (TG, DTA and DTG) were carried out in a TA instruments SDT Q600 simultaneous DTA–TGA thermal analyzer, in the temperature range 25–1100 °C, at a heating rate of 20 °C/min and with an air flow of 100 mL min^{-1}.

X-ray diffractograms (XRD) of the solids were taken in a Siemens D-500 diffractometer operating at 40 kV and 30 mA (1200 W), using filtered Cu Kα radiation and varying the angle from 2° to 65° 2θ. All the analyses were processed at a scan speed of 2° per minute.

Scanning electron microscopy (SEM) was performed using a Phillips CM 200 transmission electron microscope. Specimens for SEM analysis were prepared by grinding MAC–Nb^{5+} into finer particles, which were subsequently deposited on carbon-coated palladium films supported on 300-mesh capped grids.

Specific surface areas were determined by analyzing the nitrogen adsorption isotherms according to the BET method [10] using a physical adsorption analyzer (Micrometrics AccSorb 2100E).

Differential pulse voltammetry (DPV) measurements were accomplished in a potentiostat/galvanostat (PARC, model 273). All experiments were carried out using a conventional three-electrode cell. The working electrode was built from a PVC body with a graphite disk, which supports a carbon paste containing the sample (alumina, niobate, or Nb–alumina). The carbon paste was prepared by mixing high purity graphite (Fisher Scientific) and the samples in a 9:1.5 (w/w) ratio with a few drops of oil. Ag/AgCl was used as the reference electrode and platinum wire as the auxiliary electrode. All measurements were conducted under high purity argon. $NaBF_4$ solutions (pH 1) were employed as supporting electrolyte.

Infrared absorption spectra (FTIR) were obtained on a Perkin–Elmer 1739 spectrophotometer with Fourier transform, using the KBr pellet technique. About 1 mg of sample and 300 mg of KBr were used in the preparation of the pellets.

2.2. Antibacterial activity tests

Bacterial cultures used in the present studies were obtained from the American Type Culture Collection (ATCC). A total of seven bacterial strains were tested: *Enterococcus faecalis* ATCC 4082, *Streptococcus salivarius* ATCC 25975, *Streptococcus sanguinis* ATCC 10556, *Streptococcus mitis* ATCC 49456, *Streptococcus mutans* ATCC 25175, *Streptococcus sobrinus* ATCC 33478 and *Lactobacillus casei* ATCC 11578. These bacteria are found in the oral cavity and were selected because they are related to the development of dental caries and other mouth-related health problems.

All strains were kept in the laboratory and cryopreserved at −86 °C. They were maintained in the brain-heart infusion (BHI) broth containing 20% (v/v) glycerol at −80 °C. The mouth microbiota comprises over 700 bacterial species, detected by molecular methods, but 50% of these species have not yet been cultured in the lab [11].

2.3. Preparation of inoculums

All the bacterial strains mentioned above were incubated at 37 ± 0.1 °C for 24 h in BHI agar. Standardization of each bacteria suspension was carried out at a wavelength (λ) of 625 nm by means of a spectrophotometer, to match the transmittance of 81, equivalent to 0.5 McFarland scale (1.5×10^8 CFU mL^{-1}).

2.4. Antibacterial assay by the agar diffusion (AD) method

The antibacterial activity of the samples was determined by AD, using the well technique and employing the double-layer agar system [12]. Brain heart infusion agar (25 mL) was poured into each sterilized Petri dish (15 mm × 900 mm diameter). Next, a 12.5 mL portion of the BHI agar (50 °C) and 2.5 mL of each test suspension were gently mixed and poured onto a previously set layer and distributed in Petri dishes homogeneously. After solidification, the seed layer was perforated with a sterilized stainless-steel cylinder (inside diameter = 4 mm), to form the wells. The latter were located 25 mm away from the plate border and 40 mm halfway from each other. MAC–Nb^+, distilled water (negative controls), and an aqueous solution of Periogard® (0.12% w/w, positive control) were applied inside the wells. The plates were kept for 2 h at room temperature, to allow diffusion of the agents through the agar [13]. Afterwards, the plates were incubated at 37 °C under appropriate gaseous condition (*E. faecalis* and *S. salivarius* – aerobiosis; *S. sanguinis*, *S. mitis*, *S. mutans*, *S. sobrinus* and *Lactobacillus casei* – in microaerophilia using the candle jar technique) for 48 h. At the end of the incubation period, inhibition zones formed on the medium were measured in mm. The inhibitory zone was considered the shortest distance (mm) from the outside margin of the well to the initial point of microbial growth. Three replicates were accomplished for each bacterium.

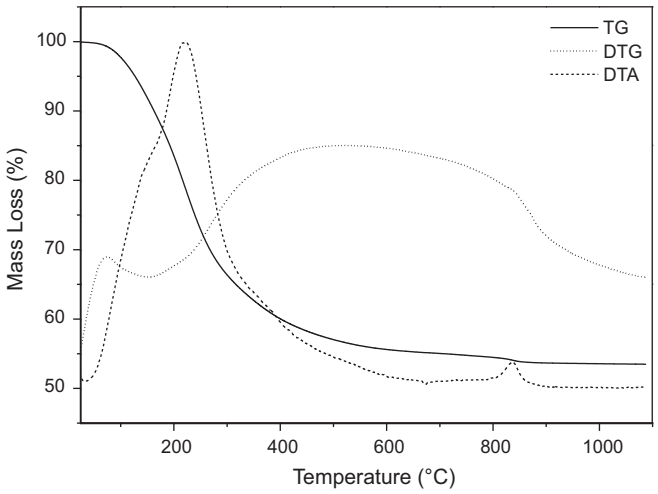

Fig. 1. TG, DTG, and DTA curves of MAC–Nb^{5+} performed in air atmosphere.

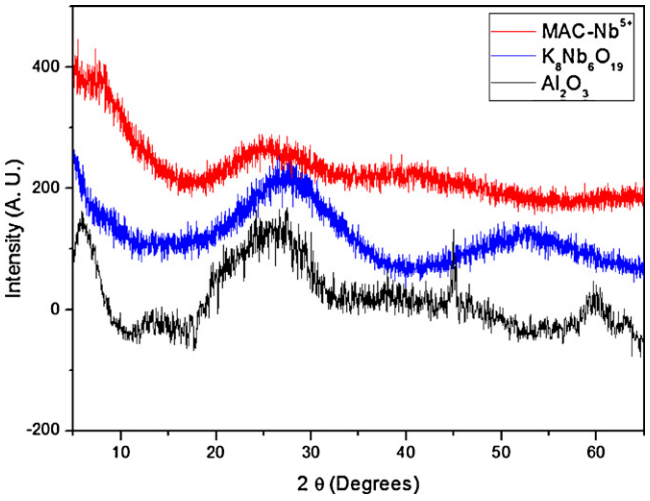

Fig. 2. Powder X-ray diffraction patterns (2θ 2–65°) of alumina, $K_8Nb_6O_{19}$ and MAC–Nb^{5+}.

2.5. Antibacterial assay by the minimum inhibitory concentration (MIC) method

The MIC determination for MAC–Nb^{5+} was carried out by the microplate dilution method [14]. Colonies from tryptic soy agar (TSA) supplemented with 5% blood sheep plates were suspended in 10.0 mL sterile tryptic soy broth (TSB). The samples were dissolved in DMSO at 1 mg mL^{-1} and then diluted in tryptic soy broth, so that concentrations in the range 400–20 μL mL^{-1} would be achieved. The final DMSO concentration was 3% (v/v), and this solution was used as negative control (concentrations ranging from 3 to 1%). The microbial suspension, TSB (100 μL), and MAC–Nb^{5+} were poured into a sterilized microplate. Chlorhexidine dihydrochloride (concentrations ranging from 0.115 to 5.9 μg mL^{-1}) was used as positive control. After 24 h incubation at 37 °C, 0.02% resazurin aqueous solution (30 μL) was poured into each microplate reservoir. The development of a red color was interpreted as positive growth, whereas the appearance of a blue color was considered negative growth. The results are expressed as MIC, i.e., the minimum concentration which prevented visible bacteria growth (blue color). Triplicate experiments were performed for each bacterium.

3. Results and discussion

3.1. Thermal analysis (TG, DTA and DTG)

The thermal analysis of MAC–Nb^{5+} is depicted in Fig. 1. The thermogravimetric analysis in air atmosphere gave evidence of 50% mass loss (w/w), mainly between 50 and 600 °C. The first step of mass loss occurring between 25 and 170 °C were assigned to loss of weakly coordinated or adsorbed water molecules from the material. The second mass loss step, taking place between 170 and 300 °C, that were attributed to loss of water and solvent molecules trapped inside the pores, and of 300–600 °C correspond to the pyrolysis and the oxidation of residual groups [9].

3.2. X-ray diffraction (XRD)

Fig. 2 shows the typical X-ray diffraction patterns of amorphous alumina. Previous studies on alumina and aluminosilicate matrices reported by our research group have demonstrated that the non-hydrolytic sol–gel methodology furnishes amorphous materials composed by admixtures of oxides, oxihydroxides and oxychlorides at low temperatures [4,5,8], which is a good indication that no $K_8Nb_6O_{19}$ segregation occurs during the synthesis of MAC–Nb^{5+}, and that the Nb^{5+} ions are well dispersed in the respective oxide matrix. The present results reveal that the structure of alumina does not change upon incorporation of Nb^{5+} ions. The peaks relative to the niobate phase appear at 27.0° and 54.0° and are also present in the XRD of MAC–Nb^{5+}. Additionally, the characteristic peaks in the XRD measurements suggest the existence of niobium and amorphous alumina phases, and the significant difference observed among the XRD patterns of MAC–Nb^{5+}, niobate and amorphous alumina confirm the presence of new phases consisting of Al_2O_3–Nb^{5+}.

3.3. Scanning electron microscopy (SEM)

The micrograph of the MAC–Nb^{5+} particles is rough and irregular, with sizes lying between 200 and 333 μm. In addition, the grain size of the doped samples decreased with the presence of Nb^{5+} such was previously reported by Hsu [15]. The particles of MAC–Nb^{5+} obtained by sol–gel route when compared with Pechini's and combustion methods shows morphology more homogeneous. Also, adhesion of particulates to the surface of larger particles, probably due to the maceration and/or grinding processes, is detected, as seen in Fig. 3.

3.4. Infrared absorption (FTIR)

The infrared absorption spectra of alumina and the MAC–Nb^{5+} matrix are displayed in Fig. 4.

According to Colomban [16], the band relative to torsional vibrational frequencies at 1640 cm^{-1} and the OH stretching bands at 3600 cm^{-1} evidence the presence of water due to the hydrated forms of alumina. Vázquez et al. [17] have studied the vibrational modes of alumina at frequencies higher than 1000 cm^{-1} and have ascribed bands around 1555 cm^{-1} and the weak band at 1100 cm^{-1} to Al–OH stretching and Al–O, respectively.

On the basis of this study, we compared the FTIR spectrum of the matrix containing the Nb^{5+} ion prepared by the non-hydrolytic sol–gel route (MAC–Nb^{5+}) with that of the alumina matrix without Nb^{5+} (blank). The bands typical of the Al–OH bonds around 1436 cm^{-1} are shifted to 1453 cm^{-1}. This demonstrates that an interaction takes place between Nb^{5+} and the alumina matrix via the hydroxyl groups, to which the Nb^{5+} ions might be coordinated. In other words, the Nb^{5+} ions might be coordinated to the hydroxyls present either on the surface or in the interior of the matrix pores. The band characteristic of the matrix Al–O bonds centered at 1105 cm^{-1} is shifted to lower wavenumber, 1072 cm^{-1}, in the

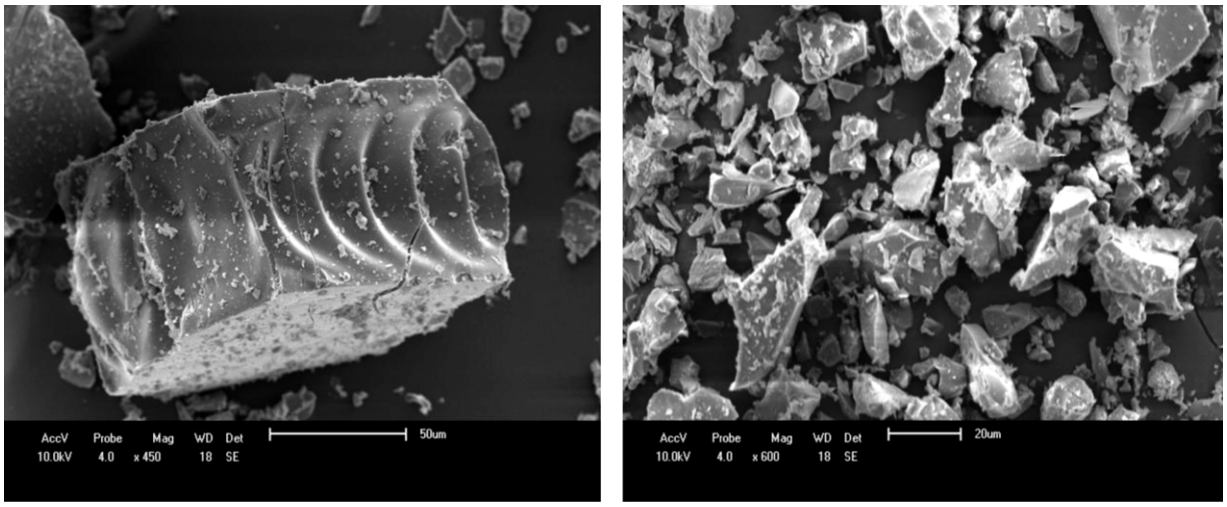

Fig. 3. SEM micrograph of MAC–Nb^{5+} at 450× (A) and 600× (B) magnification.

case of MAC–Nb^{5+}. This displacement is a result of the interaction between the coordinated Nb^{5+} and the alumina structure, thereby affecting the matrix Al–O bond stretching.

Another modification that can also occur in the matrix concerns the stretching vibrations of the condensed octahedral AlO_6 and tetrahedral AlO_4, with bands centered at 601 cm^{-1} and 970 cm^{-1}, respectively. In the case of the MAC–Nb^{5+} matrix, these bands are shifted to 584 cm^{-1} and 930 cm^{-1}, respectively, demonstrating incorporation of the Nb^{5+} ions into the alumina matrix.

Thus, it can be concluded that the niobium present in the alumina matrix can interact with the support by means of coordinative binding on the surface and/or inside the pores, or it may substitute some aluminum atoms in the structure by displacement of the existing AlO_6 and AlO_4 groups. The band assignments are summarized in Table 1.

3.5. Surface area and pore size

The surface properties and pore size of alumina (blank) and MAC–Nb^{5+} were determined by the BET method, using nitrogen adsorption.

The BET results, Table 2, demonstrate that surface area decreases with the presence of niobium ions, indicating that these ions do not contribute to any surface are to the alumina, this can be attributed to the fact that the niobium ions on surface of alumina are blocking the alumina pores reducing the space for adsorption of nitrogen as previously reported in by Khattak et al. [18] for a series of metal doped alumina.

The BET results, Table 2, also demonstrate that the employed synthetic route furnished materials with a surface area of approximately 239 $m^2\,g^{-1}$. These values are superior (230 × 197 $m^2\,g^{-1}$) to those obtained for related Nb_2O_5–Al_2O_3 materials, prepared by Somma et al. [19] using the hydrolytic sol–gel methodology. As for pore size, MAC–Nb^{5+} consists of mesopores and has high surface area, which is particularly interesting for antibacterial applications.

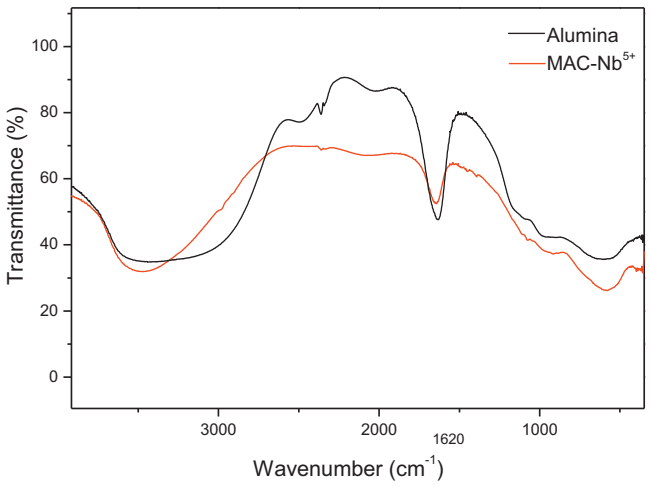

Fig. 4. Infrared absorption spectra of alumina and MAC–Nb^{5+}.

Table 1
Assignments of infrared absorption bands of alumina and MAC–Nb^{5+}.

Assignment	Al_2O_3 (cm^{-1})	MAC–Nb^{5+} (cm^{-1})
AlO_6 condensed	601	584
AlO_4 condensed	970	930
Al–O	1105	1072
Al–OH	1436	1453
H–O–H	3295, 1629	3498, 1649

3.6. Differential pulse voltammetry (DPV)

In pursuit of more information on Nb–alumina, an electrochemical study was performed, in order to evaluate the redox process in the systems neat alumina, niobate, and MAC–Nb^{5+} by differential pulse voltammetry.

The DPV profiles for alumina, the Nb-precursor, niobate, and MAC–Nb^{5+} were recorded from +1 to −2.2 V (vs Ag/AgCl). Fig. 5 (curve 1) illustrates the DPV for MAC–Nb^{5+} at pH 1, where a cathodic peak (E_{pc1}) at −0.77 V and another one at −1.4 V (E_{pc2}) vs Ag/AgCl can be observed. Additionally, two peaks appear in the range −1.8 to −2.0 V. Fig. 5 (curves 3 and 3) presents the DPV obtained for the Nb-precursor and potassium niobate ($K_8Nb_6O_{19}$). As shown in the voltammogram of MAC–Nb^{5+}, each compound illustrate a redox process at the same potential values (curves 3

Table 2
Textural properties of the samples.

Sample	BET surface area (m^2/g)	Pore volume (cm^3/g)
MAC–Nb^{5+}	239 ± 1	0.13 ± 0.001
Alumina	308 ± 1	0.16 ± 0.001

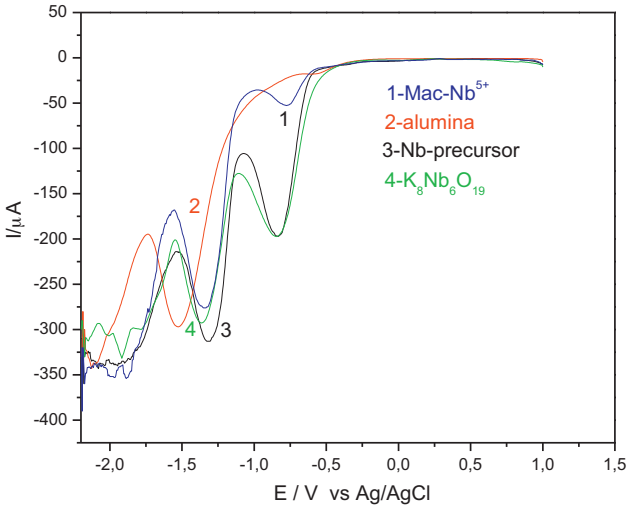

Fig. 5. Differential pulse voltammograms of MAC–Nb^{5+} (1) alumina (2), Nb-precursor (3), and niobate ($K_8Nb_6O_{19}$) (4) in aqueous solutions ($\nu = 100$ mV s^{-1}). Cathodic scan.

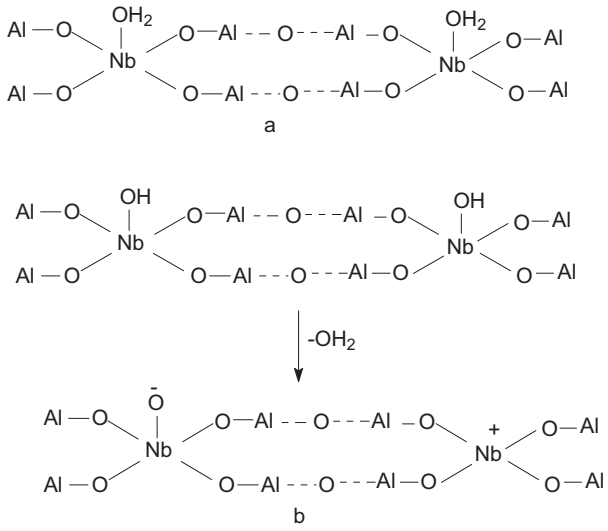

Scheme 1. Nb–Al–O interaction in MAC–Nb^{5+} at pH 1 (a) and pH 7 (b).

and 3). The DPV obtained for alumina displays a peak at −1.53 V, assigned to the Al^{3+} redox process in alumina (curve 2).

In analogy with the curves achieved for the Nb-precursor and niobate, the wave at −0.77 in the DPV of MAC–Nb^{5+} can be assigned to the Nb^{5+} reduction process as well as that at −1.4 V. Furthermore, the interactions between Nb and alumina can be confirmed by the low current intensity ratio (I_{pc1}/I_{pc2}) of the cathodic peaks obtained at −0.77 V and −1.4 V (curve 1) if compared with the ratio of neat niobate and the Nb-precursor (Fig. 5) (curves 3 and 4).

Taking into account these data and the profiles of the pulse differential voltammetry for the cathodic scan of MAC–Nb^{5+}, it is reasonable to consider that the redox process involves Nb–O–Al, as shown in Scheme 1a. The results from the infrared absorption spectra of alumina and the MAC–Nb^{5+} matrix are consistent with this interaction. The DPV profiles are pH-dependent, thus indicating the influence of an external ion. At pH 7, it is reasonable to propose that OH is coordinated to Nb (Scheme 1b).

3.7. Biological assays

3.7.1. Results from the antibacterial assays by the agar diffusion method

Since the main bacteria associated with caries are *S. mutans* and *Lactobacillus* sp [20,21], they were selected for evaluation of the possible antibacterial activity of MAC–Nb^{5+}, carried out by the AD (well technique) and broth microdilution methods, with determination of the MIC. It is expected that the search for alternative materials that inhibit bacteria growth will lead to the development of reliable alternative approaches, thereby contributing to improved oral health among the Brazilian population. This might also result in new measures for the prevention and treatment of oral cavity diseases, which are also involved in other diseases of the human body.

3.7.2. AD method (well technique)

Results from the biological assay using the AD method and MAC–Nb^{5+} *in vitro* demonstrate that this material displays antibacterial activity against all the tested bacteria, as summarized in Table 3.

Table 3 reveals that MAC–Nb^{5+} is most active against *S. mitis* and *S. sobrinus*.

The AD method shows that inhibition halos larger than that obtained with the positive control (Periogard®) are achieved for 86% of the evaluated bacteria, namely *S. sanguinis* (ATCC 10556), *S. mutans* (ATCC 25175), *E. faecalis* (ATCC 4082) and *S. salivarius* (ATCC 25975).

MAC–Nb^{5+} leads to a halo with 23.3 mm diameter, whereas the positive control furnishes a 29.3-mm diameter halo.

Control reactions, or blank tests, were carried out with alumina matrix containing no niobium ions, and these reactions did not lead to antibacterial activity. This fact confirms that the observed antibacterial activity is really due to the presence of niobium ions.

3.7.3. Results from the antibacterial assay by the minimum inhibitory concentration method

The MIC of MAC–Nb^{5+} was determined using the same standard strains described in item 2.2. Table 4 lists the MIC of MAC–Nb^{5+} against oral bacteria. MAC–Nb^{5+} is active against *S. sanguinis*, *L. casei*, *S. mutans*, *E. faecalis*, *S. salivarus*, *S. mitis* and *S. sobrinus*. MIC values lie between 40 μg mL^{-1} up to concentrations higher than 400 μg mL^{-1}. This method corroborates the results achieved by means of the AD method.

Table 3
Antimicrobial activity of MAC–Nb^{5+} against microorganisms present in the human oral cavity, evaluated by the agar diffusion method.

Bacterial strain	MAC–Nb^{5+}.	Alumina	Negative control	Positive control (PERIOGARD®)
Streptococcus sanguinis ATCC 10556	25.0 ± 1.00	0.00 ± 0.00	0.00 ± 0.00	22.0 ± 1.00
Lactobacillus casei ATCC 11578	23.3 ± 1.20	0.00 ± 0.00	0.00 ± 0.00	29.3 ± 0.60
Streptococcus mutans ATCC 25175	26.3 ± 0.60	0.00 ± 0.00	0.00 ± 0.00	22.3 ± 0.60
Enterococcus faecalis ATCC 4082	23.0 ± 1.00	0.00 ± 0.00	0.00 ± 0.00	17.7 ± 0.60
Streptococcus salivarius ATCC 25975	26.0 ± 1.00	0.00 ± 0.00	0.00 ± .00	18.7 ± 0.60
Streptococcus mitis ATCC 49456	27.7 ± 1.20	0.00 ± 0.00	0.00 ± 0.00	19.3 ± 0.60
Streptococcus sobrinus ATCC 33478	27.7 ± 1.20	0.00 ± 0.00	0.00 ± 0.00	23.7 ± 1.20

Mean values of the inhibition halo diameters in mm ± mean standard deviation.

Table 4
Determination of MIC in $\mu g\,mL^{-1}$ for MAC–Nb^{5+} against oral bacteria.

Compounds/microorganisms	*S. sanguinis* 10556	*L. casei* 11578	*S. mutans* 25175	*E. faecalis* 4082	*S. salivarius* 25975	*S. mitis* 49456	*S. sobrinus* 33478
MAC–Nb^{5+}	200	>400	200	>400	40	200	300
Alumina	**	**	**	**	**	**	**
#Positive control	3.688	1.844	0.922	3.688	0.922	0.922	0.922
Broth control (TSB)	*	*	*	*	*	*	*
DMSO 3% control	**	**	**	**	**	**	**

*There was no microorganism growth; **there was microorganism growth; #positive control.

MAC–Nb^{5+} is most efficient against the bacteria *S. salivarius*, with MIC 40 $\mu g\,mL^{-1}$. The material is moderately active against *S. sanguinis*, *L. casei*, *S. mutans*, *E. faecalis*, *S. mitis* and *S. sobrinus*, with MIC varying between 200 $\mu g\,mL^{-1}$ and >400 $\mu g\,mL^{-1}$. Literature works state that compounds with MIC lower than 100 $\mu g\,mL^{-1}$ are good antibacterial agents, whereas those with MIC ranging from 100 to 400 $\mu g\,mL^{-1}$ are moderately active [22,23].

As in the case of the study employing the AD method, control reactions, or blank tests, were conducted by employing alumina matrix containing no niobium ions. These blank tests yielded MIC values higher than 400 $\mu g\,mL$, thus showing that the matrix without niobium ions was not able to deactivate any of the investigated bacteria. This fact once again confirms that the observed antibacterial activity is really due to the niobium ions.

4. Conclusions

The non-hydrolytic sol–gel route was successfully employed for the preparation of MAC–Nb^{5+} with antibacterial properties. The chemical characterization showed that Nb^{5+} ions were inserted into the alumina matrix, interact with hydroxyl groups located on the matrix surface and inside the pores, and substitute some atoms in the alumina matrix, as confirmed by FTIR and DPV measurements. SEM analysis showed that particles are rough and more irregular.

The AD method demonstrated that MAC–Nb^{5+} displays antibacterial activity against bacteria present in the oral cavity. Future studies focusing on a chemical, biological and clinical approach shall be carried out for this material, due the potential application in oral care product.

After a careful review of the literature on the use of niobium in such diverse fields as the medical, biological and chemical areas, it was verified that this is the first study assessing the antibacterial potential of niobium by the AD technique and reporting on the use of the broth microdilution method for MIC determination of the niobium material. Therefore, both the chemical and biological studies carried out herein signalize novel applications of Nb^{5+}, which will possibly extend its application fields.

Acknowledgements

This work was a result of the collaboration between Unifran and UFBA and was supported by FAPESP, FAPESB, CAPES and CNPq. The authors acknowledge the niobium precursor furnished by the mining company CBMM (Companhia Brasileira de Metalurgia e Mineração).

References

[1] D. Yang, P. Yuan, J.X. Zhu, H.-P. He, J. Therm. Anal. Calorim. 89 (2007) 847–852.
[2] H. He, D. Yang, P. Yuan, W. Shen, R.L. Frost, J. Colloid Interface Sci. 297 (2006) 235–243.
[3] J. Husheng, H. Wensheng, W. Liqiao, X. Bingshe, L. Xuguang, Dent. Mater. 24 (2008) 244–249.
[4] K.J. Ciuffi, O.J. de Lima, H.C. Sacco, E.J. Nassar, J. Non-Cryst. Solids 304 (2002) 126–133.
[5] B.L. Caetano, L.A. Rocha, E. Molina, Z.N. Rocha, G.P. Ricci, P.C. Calefi, O.J. de Lima, C. Mello, E.J. Nassar, K.J. Ciuffi, Appl. Catal. A: Gen. 311 (2006) 122–134.
[6] P.H. Mutin, A. Vioux, Chem. Mater. 21 (2009) 582–596.
[7] I.M. Sadiq, B. Chowdhury, N. Chandrasekaran, A. Mukherjee, Nanomed. Nanotechnol. 5 (2009) 282–286.
[8] O.J. de Lima, D.P. de Aguirre, D.C. de Oliveira, M.A. da Silva, C. Mello, C.A.P. Leite, H.C. Sacco, K.J. Ciuffi, J. Mater. Chem. 11 (2001) 2476–2481.
[9] S. Acosta, R.J.P. Corriu, D. Leclercq, P. Lefèvre, P.H. Mutin, A. Vioux, J. Non-Cryst. Solids 170 (1994) 234–244.
[10] S. Brunauer, P.H. Emmett, E. Teller, J. Am. Chem. Soc. 60 (1938) 309–319.
[11] J.A. Aas, J.B. Paster, N.L. Stokes, I. Olsen, E.F. Dewhirst, J. Clin. Microbiol. 43 (2005) 5721–5732.
[12] D.C. Grove, W.A. Randall, Assay Methods of Antibiotics: A Laboratory Manual, Medical Encyclopedia, New York, (1955) p. 80.
[13] A.J.R Moller, Microbiological examination of root canals and periapical tissues of human teeth, methodological studies, Odontol. Tisdskrisft 74 (5 Suppl. 1) (1996) 371–380.
[14] Clinical and Laboratory Standards Institute, Methods for Dilution Antimicrobial Susceptibility Tests for Bacteria that Grow Aerobically, vol. 26[2], seventh ed., Approved Standard M7-A7, CLSI, Wayne, PA, 2006.
[15] Y.F. Hsu, Mater. Sci. Eng. A 399 (2005) 232–237.
[16] Ph. Colomban, J. Mater. Sci. 24 (1989) 3002–3010.
[17] A. Vázquez, T. López, R. Gómez, Bokhimi, A. Morales, O. Novaro, J. Solid State Chem. 128 (1997) 161–168.
[18] A.K. Khattak, M. Afzal, M. Saleem, G. Yasmeen, R. Ahmad, Colloids Surf. A 162 (2000) 99–106.
[19] F. Somma, P. Canton, G. Strukul, J. Catal. 229 (2005) 490–498.
[20] P.R. Murray, K.S. Rosenthal, G.S. Kobayashi, M.A. Pfaller, Microbiologia Médica, fourth ed., Guanabara Koogan, Rio de Janeiro, 2004, pp. 188–201.
[21] A. Thylstrup, O. Fejerskov, Cariologia Clínica, second ed., ed Santos, São Paulo, 1995, p. 421.
[22] M.A. Gondal, A. Bagabas, A. Dastageer, A. Khalil, J. Mol. Catal. A 323 (2010) 78–83.
[23] S.M. Magaña, P. Quintana, D.H. Aguilar, J.A. Toledo, C. Angeles-Chavez, M.A. Cortes, L. Léon, Y. Freile-Pelegrín, T. López, R.M. Torres Sanchez, J. Mol. Catal. A: Chem. 28 (2008) 192–199.